Epibatidine Activates Muscle Acetylcholine Receptors with Unique Site Selectivity

Richard J. Prince and Steven M. Sine
Receptor Biology Laboratory, Department of Physiology and Biophysics, Mayo Foundation, Rochester, Minnesota 55905 USA

ABSTRACT We recently showed that at desensitized muscle nicotinic receptors, epibatidine selects by 300-fold between the two agonist binding sites. To determine whether receptors in the resting, activatible state show similar site selectivity, we studied epibatidine-induced activation of mouse fetal and adult receptors expressed in 293 HEK cells. Kinetic analysis of single-channel currents reveals that (−)-epibatidine binds with 15-fold selectivity to sites of adult receptors and 75-fold selectivity to sites of fetal receptors. For each receptor subtype, site selectivity arises solely from different rates of epibatidine dissociation from the two sites. To determine the structural basis for epibatidine selectivity, we introduced mutations into either the γ or the δ subunit and measured epibatidine binding and epibatidine-induced single-channel currents. Complexes formed by α and mutant γ(K34S+F172I) subunits bind epibatidine with increased affinity compared to $\alpha\gamma$ complexes, whereas the kinetics of $\alpha_2\beta\delta\gamma$(K34S+F172I) receptors reveal no change in affinity of the low-affinity site, but increased affinity of the high-affinity site. Conversely, complexes formed by α and mutant δ(S36K+I178F) subunits bind epibatidine with decreased affinity compared to $\alpha\delta$ complexes, whereas the kinetics of $\alpha_2\beta\gamma\delta$(S36K+I178F) and $\alpha_2\beta\epsilon\delta$(S36K+I178F) receptors show markedly reduced sensitivity to epibatidine. The overall data show that epibatidine activates muscle receptors by binding with high affinity to $\alpha\gamma$ and $\alpha\epsilon$ sites, but with low affinity to the $\alpha\delta$ site.

INTRODUCTION

Muscle acetylcholine receptors (AChRs) are heteropentamers of homologous but functionally distinct subunits. Receptors from fetal muscle have the composition $\alpha_2\beta\gamma\delta$, whereas those from the adult contain the ϵ subunit in place of γ (Mishina et al., 1986). The receptor contains two acetylcholine (ACh) binding sites, each generated by pairs of subunits, $\alpha\delta$ and either $\alpha\gamma$ or $\alpha\epsilon$. Although early studies emphasized contributions of the α subunits to the binding sites, substantial evidence has accumulated to show that the non-α subunits also contribute to stabilization of bound ligands (reviewed in Prince and Sine, 1998a).

Owing to the presence of different non-α subunits, the $\alpha\gamma$, $\alpha\delta$, and $\alpha\epsilon$ interfaces confer distinct agonist and antagonist affinities for binding sites of fetal and adult receptors. Kinetic analysis of single-channel currents shows that ACh activates *Torpedo* (Sine et al. 1990) and fetal mouse (Zhang et al., 1995) receptors with 100- and 30-fold site selectivity, respectively. On the other hand, adult receptors from human or mouse show either less or undetectable site selectivity (Ohno et al., 1996; Akk et al., 1996; Wang et al., 1997), indicating that site selectivity depends on species and subtype of the non-α subunits. Site selectivity also depends on functional state, because desensitized receptors show no site selectivity for the classical agonists ACh and carbamylcholine (Sine and Claudio, 1991; Sine et al., 1995a). However, the novel alkaloid epibatidine, which has fM-pM affinity for certain neuronal nicotinic receptors (Gerzanich et al., 1995; Sullivan et al., 1994), selects between sites of desensitized muscle receptors, binding 300-fold more tightly to the $\alpha\gamma$ or $\alpha\epsilon$ sites than to the $\alpha\delta$ site (Prince and Sine, 1998b).

Here we use single-channel recording to delineate molecular steps underlying the activation of muscle AChRs by (−)-epibatidine. Kinetic analysis of single-channel events reveals that epibatidine selects between binding sites of resting, activatible receptors by 75-fold in the fetal subtype and 15-fold in the adult subtype. We further show that the $\alpha\delta$ interface forms the low-affinity binding site, whereas the $\alpha\gamma$ and $\alpha\epsilon$ interfaces form high-affinity sites. Thus epibatidine activates muscle AChRs with site selectivity opposite that of ACh, and maintains the same site selectivity for both activatible and desensitized states.

MATERIALS AND METHODS

Materials

[^{125}I]-labeled α-bungarotoxin was purchased from DuPont NEN (Boston, MA). (−)-Epibatidine and proadifen were purchased from Research Biochemicals Incorporated (Natick, MA). A plasmid encoding green fluorescent protein (pGreen Lantern) was purchased from Gibco (Gaithersburg, MD). Sources of AChR subunits were as previously described (Sine, 1993).

Expression of receptor complexes

We transiently transfected 293 HEK cells at ~50% confluence, using calcium phosphate precipitation (Sine, 1993). For patch-clamp studies, cells were transfected with mouse α, β, δ, either γ or ϵ, and pGreen Lantern cDNAs in the ratio 2:1:1:1:0.4. For each 35-mm plate of cells we used 2.7 μg of the α subunit cDNA. For expression of intracellular complexes, the transfection mixture included α plus either γ, δ or mutant subunits in the ratio 1:1.3. For all binding studies, 13.5 μg of α cDNA was used per 10-cm

Received for publication 23 April 1998 and in final form 24 June 1998.

Address reprint requests to Dr. Richard J. Prince, School of Biological Sciences, G-38 Stopford Building, University of Manchester, Oxford Road, Manchester M13 9PT, England. Tel.: 44 (0)161 275 5440; Fax: 44 (0)161 275 5600; E-mail: richard.prince@man.ac.uk.

0006-3495/98/10/1817/11 $2.00

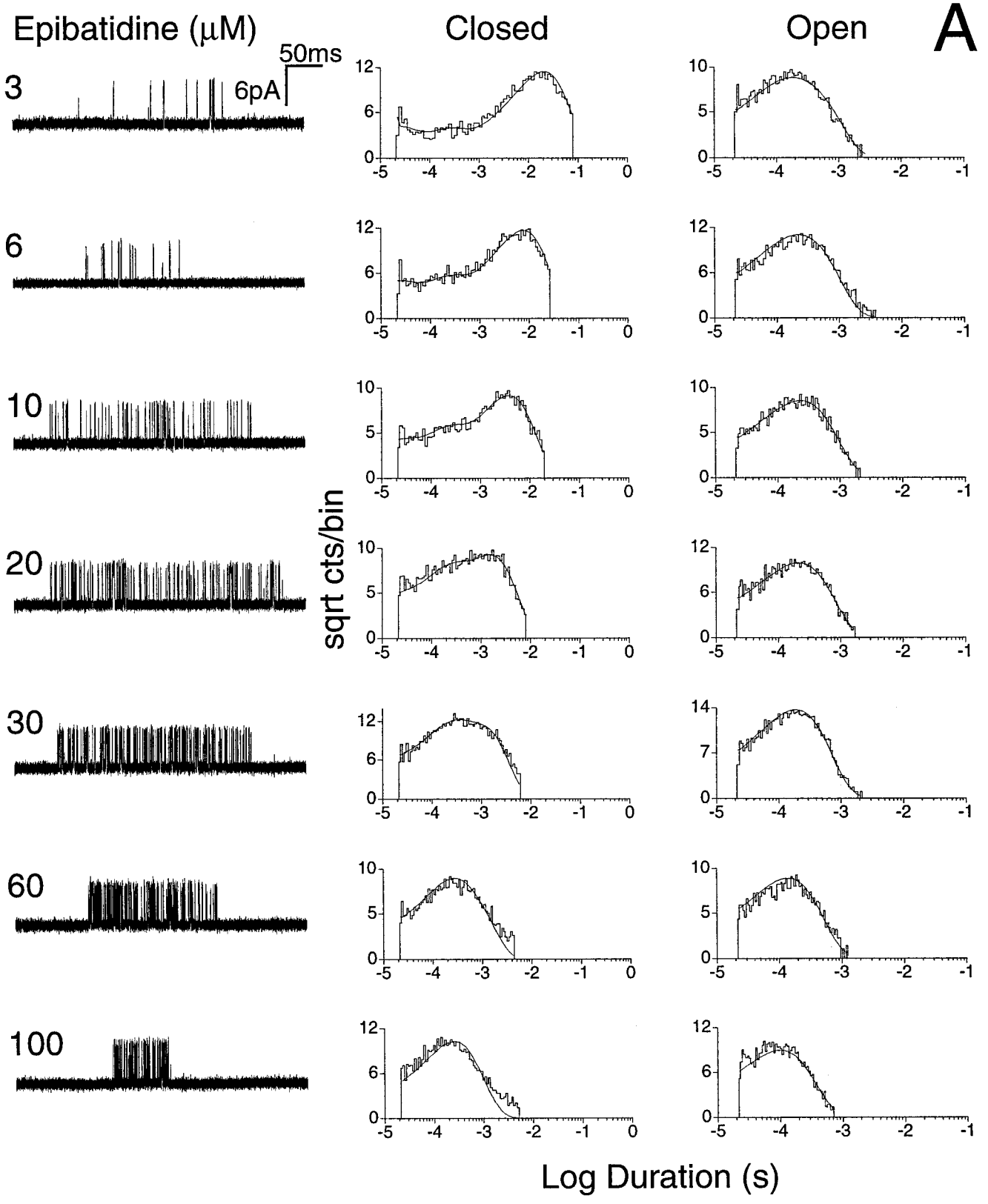

FIGURE 1 Kinetics of activation of fetal and adult AChRs by epibatidine. Left panels show traces of individual clusters from (*A*) adult and (*B*) fetal receptors recorded at the indicated concentrations of epibatidine. The traces are displayed at bandwidths of 9 kHz for the fetal receptor and 10 kHz for the adult receptor. The smooth curves through the open and closed time histograms are theoretical probability density functions calculated from the fitted rate constants for Scheme 2, with values given in Table 2.

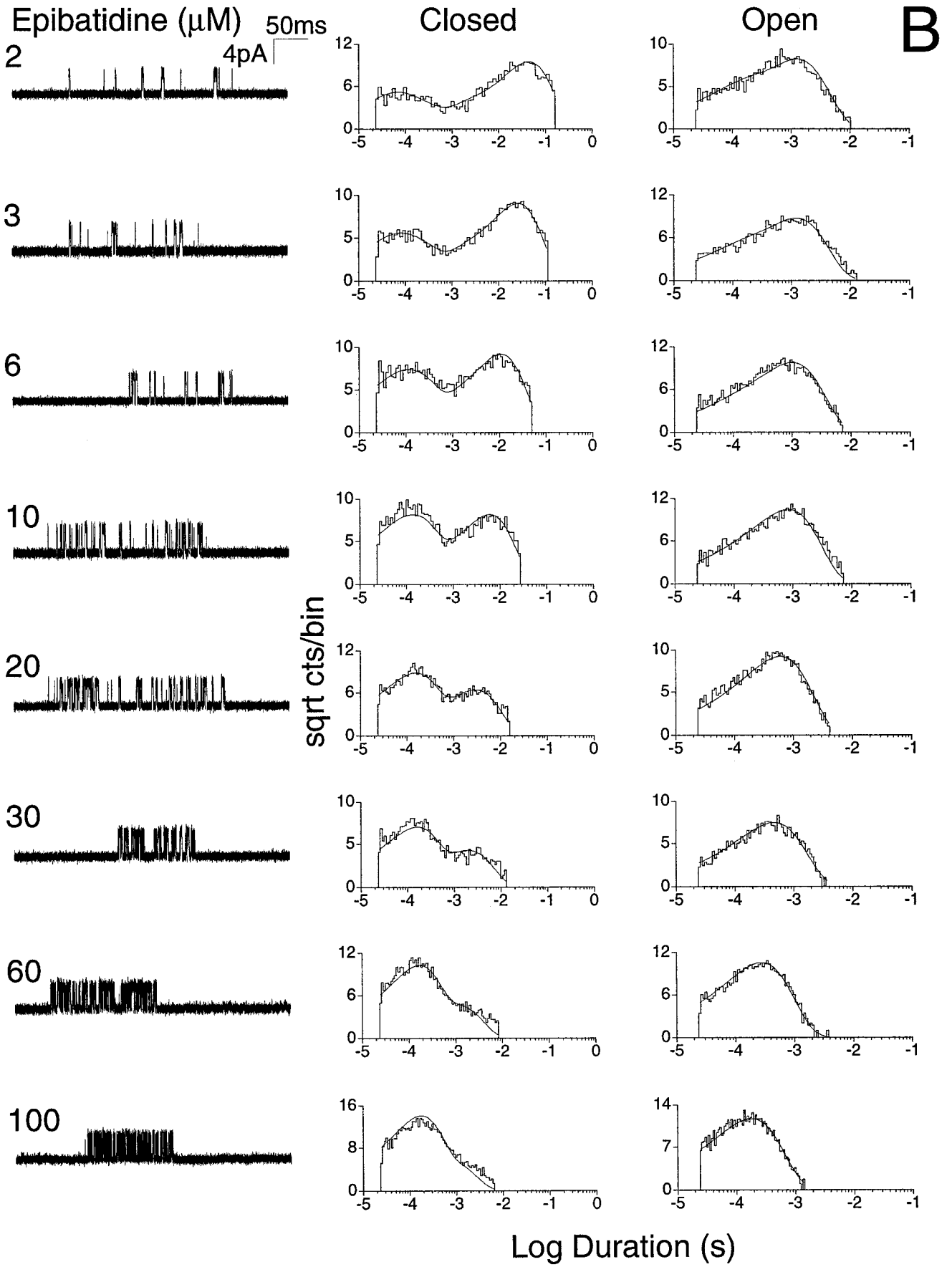

FIGURE 1 Continued.

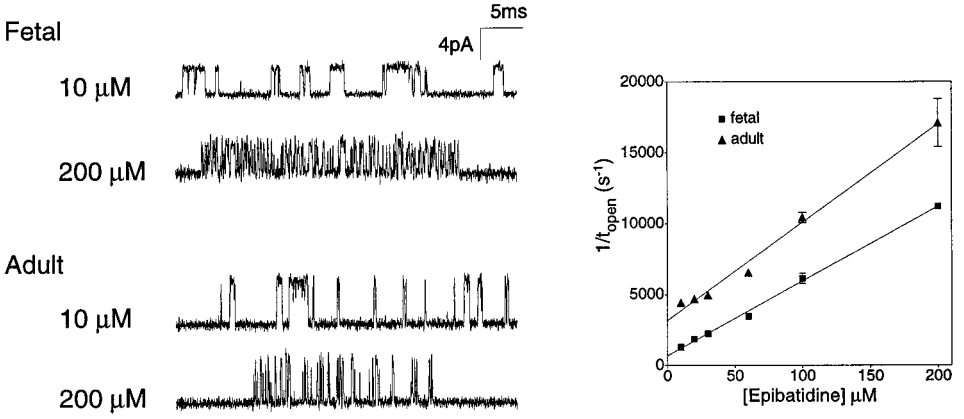

FIGURE 2 Open channel block of fetal and adult AChRs by epibatidine. t_{open} is the mean open time at the indicated concentrations of epibatidine. The traces are displayed at bandwidths of 9 kHz for the fetal receptor and 10 kHz for the adult receptor. The data are fit by the equation $1/t_{open}$ = [epibatidine] · k_{+b} + α', where k_{+b} is the association rate for epibatidine at the channel block site and α' is the apparent channel closing rate. The derived parameters are given in Table 1.

plate. After incubation in the DNA/calcium phosphate medium for 12–16 h, the medium was replaced with normal growth medium. For patch-clamp studies the cells were maintained for a further 12–24 h at 37°C, and for 36–48 h for binding studies.

Patch-clamp recordings

Single-channel currents were recorded in the cell-attached configuration as previously described (Wang et al., 1997). Transfected cells were identified under fluorescence optics by their expression of green fluorescent protein. All recordings were obtained at a membrane potential of −70 mV and a temperature of 23–25°C. Both bath and pipette solutions contained (in mM) 142 KCl, 5.4 NaCl, 1.8 $CaCl_2$, 1.7 $MgCl_2$, and 10 HEPES (pH 7.4). Epibatidine was included in the electrode solution at specified concentrations. Single-channel currents were recorded with an Axopatch 200A amplifier at an initial bandwidth of 50 kHz. Currents were digitized using an ITC-16 analog-to-digital interface at a sampling rate of 6 μs and recorded to the hard disk of a Power Macintosh 7100 with the program Acquire (Bruxton Corporation, Seattle, WA). Data were acquired during periods of receptor activation by triggering currents exceeding 40% of the typical amplitude of the channel being studied, and acquisition was initiated 300 ms before the triggering event and terminated 300 ms after the last triggering event. Currents were detected at a final bandwidth of 9 kHz (fetal receptor) or 10 kHz (adult receptor) by the half-amplitude criterion, using TAC 2.51 (Bruxton Corporation). Open and closed duration histograms were constructed and fit by the sum of exponentials, using TACFIT (Bruxton Corporation).

TABLE 1 Kinetic parameters derived from analysis of open channel block

	k_{+b} (μM^{-1} s^{-1})	k_{-b} (s^{-1})	α' (s^{-1})
Fetal	52.5 ± 1.4	5591 ± 168	695 ± 114
Adult	69.2 ± 3.3	4313 ± 402	3183 ± 321
αβδγ(K34S+F172I)	49.3 ± 0.4	5445 ± 369	323 ± 21
αβγδ(S36K+I178F)	50.6 ± 1.6	6804 ± 93	1122 ± 312
αβεδ(S36K+I178F)	54.9 ± 8	6181 ± 716	5360 ± 1560

k_{+b} and α' were calculated by linear regression to the equation $1/t_{open}$ = [epibatidine] · k_{+b} + α', where k_{+b} is the association rate for epibatidine at the channel block site and α' is the apparent channel closing rate. For wild-type receptors and αβδγ(K34S+F172I), k_{-b} is the mean of $1/t_{block}$ at 100 μM epibatidine, where t_{block} is the time constant of the closings corresponding to channel block. For αβγδ(S36K+I178F) and αβεδ(S36K+I178F), k_{-b} was calculated using data obtained at 60 μM and 100 μM epibatidine. All parameters are expressed ± SE, with errors derived from linear regression. For wild-type and αβδγ(K34S+F172I) receptors at least three determinations were made at each concentration, with each replicate treated independently in the regression analysis. For receptors containing δ(S36K+I178F), data are from single experiments.

At the epibatidine concentrations used in this study, events corresponding to activation of a single channel were identified as clusters of closely spaced openings preceded and followed by long closings. Cluster boundaries were defined as any closings longer than the duration at which the main component of closings in the histogram intersected the succeeding closed time component. For example, at 3 μM epibatidine, the main component of closings had a time constant of 20–30 ms, the succeeding component had a time constant of 100–150 ms, and cluster boundaries were typically defined as closings of 100 ms or longer. An unavoidable consequence of defining clusters of channel activity in this manner is that we cannot account for trailing and leading closed times, i.e., the closed dwell times that occur after the receptor recovers from desensitization, but before the channel opens, and those that occur between the last opening in a cluster and entry of the receptor into the desensitized state. We dealt with this problem in two ways. First, we deleted the final opening in each apparent cluster to yield equal numbers of openings and closings. Second, only clusters containing 10 or more openings were included in the analysis. Using this method, we expect the cluster open probability (P_{open}) to be overestimated by a maximum of 10%. However, the true error is likely to be much lower, because even at the lowest concentrations of epibatidine, clusters contained an average of 30–40 openings. At lower concentrations of epibatidine there is less desensitization and therefore a greater number of active channels in the patch. Therefore, to minimize errors in assigning cluster boundaries at low concentrations of epibatidine, we analyzed only recordings from patches with lower channel activity. Any clusters in which two receptors opened simultaneously were rejected. For each cluster within a recording, we calculated the p_{open} and mean open duration (t_{open}) and plotted their distributions to determine kinetic homogeneity. Both P_{open} and t_{open} distributions typically consisted of one major component, of roughly Gaussian shape, with small contributions from clusters with very different kinetic properties. All clusters with P_{open} and t_{open} within two standard deviations of the mean of the major distribution were selected for further analysis. Selection typically included ~80% of the original clusters. Selected clusters were transferred to an IBM RS6000 computer and analyzed with the program MIL (Qin et al., 1996). MIL calculates the likelihood of obtaining the observed distributions of open and closed durations given a particular kinetic scheme (for schemes see Results), and maximizes the likelihood by optimizing the rate constants in the scheme. For the fetal receptor we included recordings at 2, 3, 6, 10, 20, 30, 60, and 100 μM (−)-epibatidine in the analysis, and for the adult-type receptor 3, 6, 10, 20, 30, 60 and 100 μM. After fitting, the probability density function computed from the kinetic scheme and the derived rate constants (Qin et al., 1996) was superimposed on the experimental dwell time histograms.

TABLE 2 Kinetic parameters for epibatidine activation of adult, fetal, and $\alpha\beta\delta\gamma$(K34S+F172I) receptors

		k_{+1}	k_{-1}	K_1 (μM)	k_{+2}	k_{-2}	K_2 (μM)
Adult	Scheme 1	375 ± 30	3726 ± 400	10	331 ± 9	49400 ± 1500	149
	Scheme 2	300 ± 21	3533 ± 374	11.8	356 ± 10	44200 ± 1020	124
Fetal	Scheme 1	118 ± 16	238 ± 40	2.02	113 ± 4	17700 ± 640	156
	Scheme 2	112 ± 14	231 ± 27	2.06	113 ± 3	17400 ± 564	154
$\alpha\beta\delta\gamma$(K34S+F172I)	Scheme 1	253 ± 36	39 ± 7	0.16	180 ± 3	21572 ± 477	119
	Scheme 2	248 ± 33	38 ± 5	0.15	180 ± 4	21538 ± 304	119

β_1	α_1	Θ_1	β_2	α_2	Θ_2	k_{+b}	k_{-b}	K_B (μM)
100 ± 13	10400 ± 747	0.01	9500 ± 838	3660 ± 33	2.6	77.6 ± 1	5720 ± 101	74
105 ± 14	10300 ± 746	0.01	9070 ± 814	3670 ± 63	2.47	76.8 ± 2.5	5708 ± 119	74
13 ± 1	8400 ± 740	0.002	4080 ± 200	782 ± 7	5.22	57.4 ± 0.5	6950 ± 58	121
13 ± 1	8370 ± 530	0.002	4070 ± 294	781 ± 10	5.21	57.4 ± 1	6950 ± 156	121
29 ± 1	9715 ± 281	0.003	11532 ± 477	368 ± 4	31.3	52.2 ± 0.4	6596 ± 63	126
29 ± 1	9717 ± 280	0.003	11532 ± 1057	368 ± 4	31.3	52.3 ± 1	6596 ± 89	126

Parameters were derived from maximum likelihood fitting (see Results) of single-channel data obtained at epibatidine concentrations from 3–100 μM for the adult, 2–100 μM for the fetal receptor, and 0.3–60 μM for $\alpha\beta\delta\gamma$(K34S+F172I)). Parameters are expressed ± SE. Association constants are given in units of $\mu M^{-1}\ s^{-1}$, and all others in units of s^{-1}. Schemes 1 and 2 are defined in the text.

Ligand binding measurements

Epibatidine binding to intracellular complexes was performed as previously described (Prince and Sine, 1996). The following form of the Hill equation was fitted to the binding data:

$$1 - \text{fractional occupancy} = 1 - [A]^n/([A]^n + K_{app}^n) \qquad (1)$$

where [A] is the agonist concentration, n is the Hill coefficient, and K_{app} is the apparent dissociation constant.

RESULTS

Basic observations

To investigate the kinetics of receptor activation by epibatidine, we recorded single-channel currents from 293 HEK cells transfected with α, β, δ, and either γ (fetal receptor) or ϵ (adult receptor) subunits. At (−)-epibatidine concentrations from 2 μM to 200 μM (fetal receptor) or 3 μM to 200 μM (adult receptor), single-channel currents appear in clearly defined clusters (Fig. 1). Each cluster begins with the transition of a single receptor from the desensitized to the activatible state, followed by a period of channel activity, and then terminates by return to the desensitized state. Previous work established that the kinetics of activation can be investigated by analyzing single-channel activity within identified clusters (Sakmann et al., 1980; Sine and Steinbach, 1987; Sine et al., 1990). Thus for each epibatidine concentration we constructed open and closed time histograms of events within clusters.

Considering first the intracluster closed time histograms, both fetal and adult receptors exhibit two or three discernible peaks, or exponentials, depending on epibatidine concentration (Fig. 1). At low concentrations of epibatidine, the longer of these exponentials dominates (time constant ~30 ms at 3 μM) and moves to briefer durations as the epibatidine concentration is increased. The second major component (time constant ~0.2 ms) contributes little to the closed time histogram at low concentrations, but its fractional area increases with increasing concentration. The time constant of this second component remains unchanged across the range of epibatidine concentrations. The third and briefest component (time constant 20–50 μs) is separated from the other components only at epibatidine concentrations less than 20 μM; at higher concentrations it is masked by the growing envelope of 0.2-ms closings.

Turning to the open time histograms, the major component of long openings is accompanied by a briefer component with fractional area that decreases with increasing epibatidine concentrations (less than 10 μM epibatidine). The concentration dependence of brief and long openings suggests that they correspond to receptors with one and two sites occupied by epibatidine, respectively. In addition, for both fetal and adult receptors, the mean duration of long openings decreases with increasing epibatidine concentrations.

The basic observations indicate an activation process driven by epibatidine concentration, plus open channel block by epibatidine. Considering first open channel block, its hallmarks are a concentration-dependent decrease in mean open time, a concentration-dependent increase in the fractional area of one closed time component, and constant mean duration of the corresponding closed intervals across all blocker concentrations. Accordingly, mean open time t_{open} depends on epibatidine concentration thus:

$$1/t_{open} = [A] \cdot k_{+b} + \alpha'$$

where [A] is epibatidine concentration, k_{+b} is the block association rate, and α' is the apparent channel closing rate (Neher and Steinbach, 1978). α' is expected to be slower than the true closing rate, α, because bandwidth limitations prevent resolution of very brief channel closings. For both fetal and adult receptors, $1/t_{open}$ increases linearly with increasing epibatidine concentration (Fig. 2). The ordinate intercept gives the closing rate constant, which is faster for adult than for fetal receptors (Table 1). The mean blocked

time t_{block} gives the reciprocal of the unblocking rate constant, k_{-b}, which was calculated from the time constant of the major closed time component at 100 μM epibatidine, where channel blocking events dominate (Table 1).

Maximum likelihood fitting

To derive individual rate constants for steps underlying activation by epibatidine, we analyzed open and closed durations according to the following standard kinetic scheme:

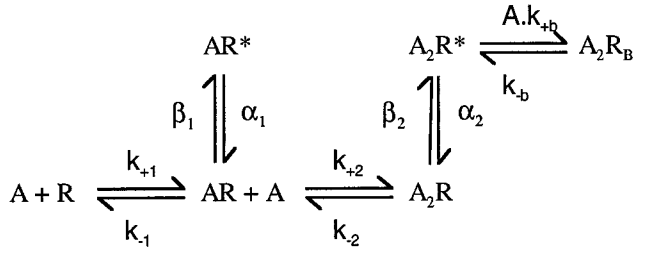

Scheme 1

where k_{+1}, k_{+2}, and k_{+b} are association rate constants for agonist (A); k_{-1}, k_{-2}, and k_{-b} are dissociation rate constants; R is the closed state of the receptor; R* is the open state; and R_B is the blocked state. β and α are channel opening and closing rate constants, respectively. To test the possibility that epibatidine binds independently to the two sites, we also fit the following expanded scheme to the data:

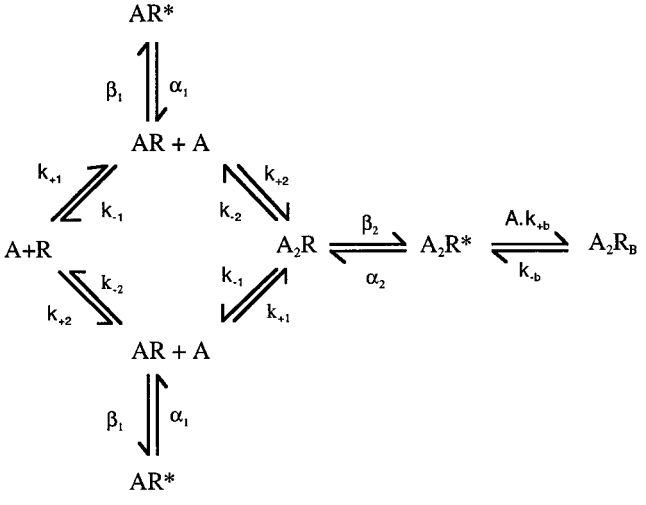

Scheme 2

Predictions of Scheme 2 differ from those of Scheme 1 by the presence of an additional closed time component. However, when k_{-1} and k_{-2} are very different, Schemes 1 and 2 are equivalent because transition out of the A_2R state almost always occurs through the pathway with the faster dissociation rate constant. To estimate the set of activation rate constants for epibatidine, we fit predictions of Schemes 1 and 2 to the data with the program MIL. MIL computes the likelihood of the experimental series of open and closed times given a set of trial rate constants, and changes the rate constants to maximize the likelihood (Qin et al., 1996).

Our fitting analysis typically includes dwell times obtained across the entire range of agonist concentrations. However, because of open channel block by epibatidine, we analyzed the data in two steps. First we fit the schemes to data obtained at epibatidine concentrations from 2 μM through 20 μM. Here we constrained k_{+b} and k_{-b} to values obtained from analysis of channel block described above (Fig. 2 and Table 1), but allowed the remaining parameters to vary freely. Our rationale is that determining parameters associated with occupancy of monoliganded receptors (k_{+1}, k_{-1}, β_1, and α_1) depends on temporal separation of mono- and diliganded openings, whereas parameters associated with channel opening (β_2) depend on temporal separation of very brief (20–50 μs mean) and long closings (~30 ms mean at 3 μM epibatidine). Furthermore, excessive channel block interferes with the temporal resolution of these components, either by masking the closed times or by decreasing the open times. Thus favorable conditions for fitting are achieved at epibatidine concentrations from 2 μM through 20 μM. Results from this preliminary fit yielded well-defined estimates of β_2, k_{+1}, k_{-1}, β_1, and α_1, and theoretical probability density functions that closely matched our experimental data, similar to the fitted histograms in Fig. 1.

The second round of fitting included data obtained at 2–100 μM (fetal receptor) or 3–100 μM (adult receptor) epibatidine. Because kinetic steps associated with occupancy of the first binding site are obscured by channel block and are less frequent at high epibatidine concentrations, the second round of fitting constrained k_{+1}, k_{-1}, β_1, α_1, and β_2 to values obtained in the first round of fitting, but allowed k_{+2}, k_{-2}, α_2, k_{+b}, and k_{-b} to vary freely. For both adult and fetal receptors, fitting either Scheme 1 or 2 to the data yields well-defined parameters, which are essentially identical for the two schemes (Table 2). We also tried fitting in one stage with all parameters free to vary, and found rate constants within twofold of those estimated by fitting in two stages (not shown); the differences likely arise from overrepresentation of blocking events in the one-stage fitting. The fitted probability density functions calculated from Scheme 2 superimpose on the experimental histograms for epibatidine concentrations up to 60 μM. At 100 μM epibatidine, a small excess of long closings is present, perhaps because of the averaging across multiple recordings inherent in global fitting, or to an additional class of closings not considered in Schemes 1 and 2. Finally, values of α_2, k_{+b}, and k_{-b} obtained by maximum likelihood fitting (Table 2) agree with parameters obtained by analysis of channel block (Fig. 2 and Table 1).

The fitted parameters indicate fast, nearly diffusion-limited rate constants for epibatidine association, which are equal for each binding site of each receptor type, but are approximately threefold faster for adult compared to fetal receptors (Table 2). For both fetal and adult receptors, rate constants for epibatidine dissociation differ between the two sites, and this difference is solely responsible for the different affinities of the sites. The net result of the association and dissociation rate constants is greater selectivity of epi-

batidine for sites in fetal than in adult receptors. Comparison of absolute values of the dissociation constants reveals a common low-affinity site in both receptor types, but different high-affinity sites. Observation of a common low-affinity site suggests that it corresponds to the $\alpha\delta$ site present in both fetal and adult receptors.

The fitted parameters also reveal channel opening rate constants five- to tenfold slower than for the natural transmitter ACh (Maconochie and Steinbach, 1998; Zhang et al., 1995; Wang et al., 1997), whereas channel closing rate constants are only slightly faster (Table 2). The resulting channel opening equilibrium constants are much less than observed for ACh. As observed for ACh, however, epibatidine opens fetal receptors more readily than adult receptors. Finally, although epibatidine blocks open channels with a forward blocking rate similar to that for ACh, its unblocking rate is much slower, allowing temporal resolution of channel blocking events.

As a further check of our fitted parameters, we calculated the theoretical channel P_{open} as a function of epibatidine concentration for both fetal and adult receptors. The kinetically derived P_{open} curves superimpose on the experimental data (Fig. 3), further supporting the rate constant estimates. Epibatidine activates fetal and adult receptors with similar potency, and achieves a maximum P_{open} less than 0.5. The bell shape of the P_{open} curves results from similar dissociation constants for epibatidine binding to the transmitter and the channel blocking sites.

Subunit compositions of the high- and low-affinity binding sites

We previously showed that carbamylcholine selectivity for intracellular $\alpha\gamma$ and $\alpha\delta$ complexes coincided with the selectivity of resting receptors determined by the kinetics of single-channel currents (Prince and Sine, 1996). Thus we measured epibatidine binding to intracellular $\alpha\epsilon$, $\alpha\gamma$, and $\alpha\delta$ complexes to gain insight into the subunits that form the high- and low-affinity sites in resting receptors. Epibatidine binds to intracellular complexes with the rank order $\alpha\epsilon > \alpha\gamma > \alpha\delta$ (Fig. 4 and Table 3), suggesting that resting receptors bind epibatidine with similar site selectivity. The low affinity observed for the $\alpha\delta$ site suggests that it corresponds to the common low-affinity site detected in the kinetic analysis (Table 2).

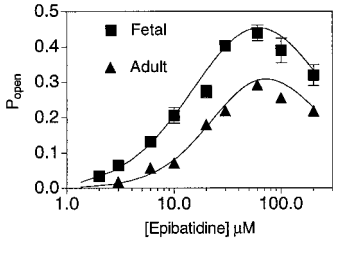

FIGURE 3 Epibatidine dose-response relationships for fetal and adult AChRs. The overall P_{open} for each recording was calculated at the indicated concentrations as described in Materials and Methods. Each point represents the mean ± SEM of the overall P_{open} values from at least three recordings. The solid lines are the theoretical P_{open} curves calculated from the fitted kinetic parameters for Scheme 2 and given in Table 2.

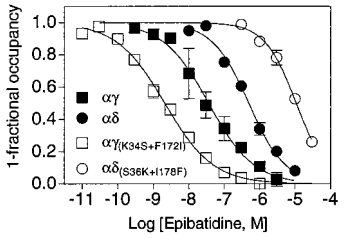

FIGURE 4 Steady-state binding of epibatidine to $\alpha\gamma$, $\alpha\delta$, $\alpha\gamma$(K34S+F172I), and $\alpha\delta$(S36K+I178F) intracellular complexes. Binding of epibatidine was measured as described in Materials and Methods. Each point is the mean of three determinations; the error bars represent the SEM. Curve fitting parameters are given in Table 3.

Epibatidine binding and kinetics of activation for receptors with mutant γ or δ subunits

To directly determine the subunits that form the high- and low-affinity sites in resting, activatible receptors, we mutated residues in either the γ or the δ subunit and compared epibatidine binding to intracellular complexes with binding parameters determined from the kinetics of single-channel currents.

We previously showed that the pairs of equivalent residues, γK34/δS36 and γF172/δI178, are major determinants of carbamylcholine and conotoxin M1 selectivity for the $\alpha\gamma$ and $\alpha\delta$ binding sites (Sine et al., 1995b; Prince and Sine, 1996). In particular, when coexpressed with the α subunit to form intracellular complexes, the double mutant γ(K34S+F172I) increases affinity for carbamylcholine, whereas δ(S36K+I178F) decreases affinity. For epibatidine, the mutations affect the affinity of intracellular complexes similarly; γ(K34S+F172I) increases affinity, whereas δ(S36K+I178F) decreases affinity (Fig. 4). Thus equipped with mutant γ and δ subunits that affect epibatidine affinity, we sought to determine the subunits that form the high- and low-affinity sites in fully assembled receptors.

We recorded single-channel currents activated by epibatidine for pentameric cell surface receptors containing either γ(K34S+F172I) or δ(S36K+I178F) plus complementary

TABLE 3 Binding of epibatidine to intracellular complexes

	K_d (nM)	n
$\alpha\gamma$	36.5 ± 6.4	0.68 ± 0.07
$\alpha\delta$	494 ± 45	0.84 ± 0.06
$\alpha\gamma$(K34S+F172I)	2.1 ± 0.2	0.64 ± 0.0
$\alpha\delta$(S36K+I178F)	10820 ± 820	0.97 ± 0.07
$\alpha\epsilon$	4.8 ± 0.7	0.76 ± 0.08

The parameters and error estimates are derived from fits of Eq. 1 to cumulated data from at least three independent experiments, with each replicate treated independently. Each fitted parameter is expressed ± SE. K_d is the apparent dissociation constant, and n is the Hill coefficient.

wild-type subunits. Coexpression of α, β, and δ with γ(K34S+F172I) increases sensitivity to epibatidine compared to wild-type receptors, whereas coexpression of α, β, and γ with δ(S36K+I178F) greatly diminishes sensitivity (Fig. 5). For receptors containing γ(K34S+F172I), single-channel kinetic analysis reveals well-defined rate constants and probability density functions that superimpose upon the experimental closed and open time histograms (Fig. 6). The fitted parameters reveal that γ(K34S+F172I) has little effect on the low-affinity site, but it increases the affinity of the high-affinity site to 150 nM (Table 2). This high affinity for resting receptors owes to a twofold increase of the association rate, and a sixfold slowing of the dissociation rate. Furthermore, epibatidine opens $\alpha\beta\delta\gamma$(K34S+F172I) receptors more efficiently than wild-type receptors, because of increased channel opening and decreased channel closing rates. We previously noted similar effects of these mutations on receptors activated by acetylcholine (Prince and Sine, 1997). Because the γ subunit harbors the mutations, we conclude that the resting state $\alpha\gamma$ site binds epibatidine with high affinity, whereas the resting state $\alpha\delta$ site binds with low affinity.

We carried out the converse experiment by coexpressing δ(S36K+I178F) with complementary subunits from either fetal or adult receptors. Receptors containing δ(S36K+I178F) show decreased sensitivity to epibatidine, as expected from a decreased affinity of the $\alpha\delta$ site (Fig. 5). However, the marked decrease in affinity prevented clear definition of clusters, and channel block further obscured events at high epibatidine concentrations. Thus kinetic analysis was not feasible for receptors containing δ(S36K+I178F). Nevertheless, the decreased sensitivity produced by δ(S36K+I178F) further supports assignment of the $\alpha\delta$ site to the resting state low-affinity site, and $\alpha\gamma$ or $\alpha\epsilon$ sites to resting state high-affinity sites.

DISCUSSION

This study uses single-channel kinetic analysis to resolve individual reaction steps underlying epibatidine-induced activation of fetal and adult muscle nicotinic receptors. Two standard and related kinetic schemes quantitatively describe the kinetics of activation over a 100-fold range of epibatidine concentrations. Our results indicate that epibatidine activates muscle receptors with unique site selectivity, binding with high affinity to $\alpha\gamma$ and $\alpha\epsilon$ binding sites but with low affinity to $\alpha\delta$ sites.

Previous studies of AChR activation demonstrated distinct binding affinities for the natural transmitter ACh at the two binding sites of the receptor, and that the distinct affinities originate from different dissociation rate constants at the two binding sites (Sine et al., 1990; Zhang et al., 1995; Ohno et al., 1996). Similarly, epibatidine binds with distinct affinities to activatible fetal and adult receptors, primarily because of differences in dissociation rate constants at the two sites. The presence of a common α subunit in the $\alpha\delta$, $\alpha\gamma$, and $\alpha\epsilon$ binding sites suggests that differences in dissociation rates are due to different contributions of the δ, γ, and ϵ subunits. Mutagenesis and affinity labeling studies indicate that four loops in each of these non-α subunits contribute to the binding sites (reviewed in Prince and Sine, 1998a), suggesting that differences in dissociation rates are due to amino acid differences in one or more of these loops. Thus structural differences in the non-α subunits may affect release of epibatidine from its final docking site or the height of an energy barrier in the pathway out of the site.

Association rate constants for full agonists approach but do not equal the theoretical diffusion limit of $\sim$1000 μM^{-1} s^{-1} (Fersht, 1985). Like full agonists, epibatidine readily enters the binding site, associating with rate constants be-

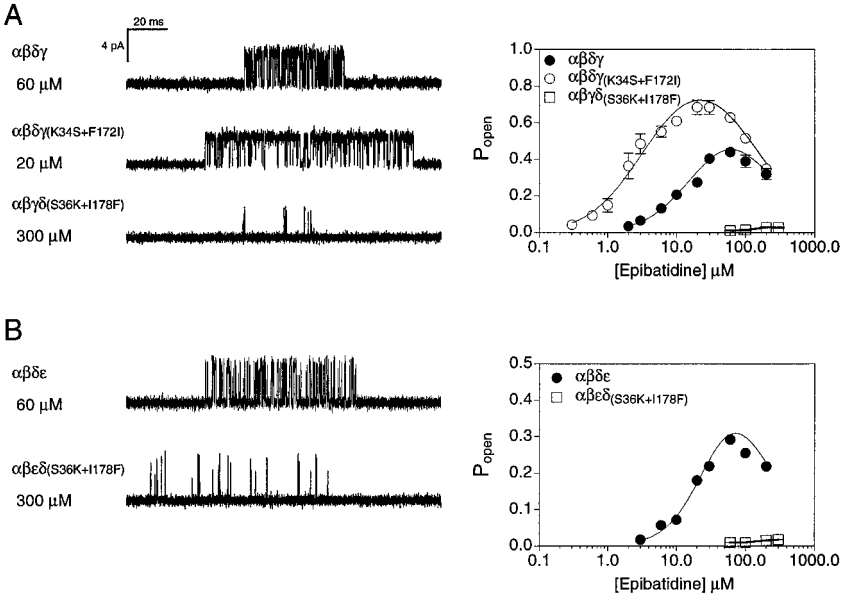

FIGURE 5 Epibatidine activation of acetylcholine receptors containing either γ(K34S+F172I) or δ(S36K+I178F) plus complementary subunits. (*A*) Fetal type receptors. (*B*) Adult type receptors. Left panels show traces of individual clusters recorded at maximally effective concentrations of epibatidine. The traces are displayed at a bandwidth of 9 kHz (fetal type) or 10 kHz (adult type). The right panels show concentration-response relationships. The overall P_{open} for each recording was calculated at the indicated concentrations as described in Materials and Methods. For wild-type and $\alpha_2\beta\delta\gamma$(K34S+F172I) receptors, each point represents the mean ± SEM of the overall P_{open} values from at least three recordings. For $\alpha\beta\epsilon\delta$(S36K+I178F) and $\alpha\beta\gamma\delta$(S36K+I178F), each point is a single determination. For wild-type and $\alpha_2\beta\delta\gamma$(K34S+F172I) receptors, the smooth curves represent P_{open} calculated from the fitted kinetic parameters for Scheme 2 and given in Table 2.

tween 100 μM and 300 $\mu M^{-1}\ s^{-1}$. These values are similar to those previously determined for ACh (Sine et al., 1990; Zhang et al., 1995; Wang et al., 1997), but are much faster than for the elementary agonist tetramethylammonium (Zhang et al., 1995). Association rate constants are very similar for both binding sites of a given receptor type, suggesting structurally similar diffusion pathways into the sites, despite their differing subunit compositions. Furthermore, global structure appears to affect association, as epibatidine associates with the $\alpha\delta$ site in the fetal receptor at 100 $\mu M^{-1}\ s^{-1}$, whereas it associates with the same site in the adult receptor at more than 300 $\mu M^{-1}\ s^{-1}$. Thus epibatidine readily diffuses into the binding sites, perhaps encountering modest structural barriers common to both sites.

Our results show that in activating the AChR, epibatidine selects between binding sites of the adult receptor by 15-fold and of the fetal receptor by 75-fold. However, kinetic analysis alone does not identify which subunits form the high- and low-affinity binding sites. For ACh and carbamylcholine, assignment of the high- and low-affinity sites relies on the observation that intracellular $\alpha\delta$ complexes bind agonist with ~30-fold higher affinity than $\alpha\gamma$ complexes (Blount and Merlie, 1989; Prince and Sine, 1996). Because this affinity difference is similar to that determined by single-channel kinetic analysis (Zhang et al., 1995), the $\alpha\delta$ site is thought to form the high-affinity activatible site in fetal AChRs.

To identify which site binds epibatidine with high affinity, we compared relative affinities of intracellular $\alpha\gamma$, $\alpha\delta$, and $\alpha\epsilon$ complexes with our kinetically determined binding affinities. Epibatidine binds to intracellular complexes with the rank order of affinity $\alpha\epsilon > \alpha\gamma > \alpha\delta$, suggesting that the $\alpha\delta$ site common to fetal and adult receptors forms the low-affinity epibatidine site (see also Prince and Sine, 1998b). Our kinetic data support a common low-affinity site, as we observe similar kinetically derived dissociation constants for the low-affinity site in fetal and adult AChRs.

To directly identify the subunits that form the high- and low-affinity sites, we examined single-channel kinetics of receptors containing mutant γ or δ subunits. Receptors containing γ(K34S+F172I) display increased sensitivity to epibatidine, whereas those containing δ(S36K+I178F) display decreased sensitivity. Kinetic analysis reveals that γ(K34S+F172I) increases the affinity of the high-affinity binding site, without affecting the low-affinity site; the increased affinity is due primarily to slowing of the rate of epibatidine dissociation. Thus our results from mutagenesis provide additional and strong support that the $\alpha\gamma$ subunit pair forms the high-affinity binding site for epibatidine, whereas the $\alpha\delta$ pair forms the low-affinity site.

We chose the mutations γ(K34S+F172I) and δ(S36K+I178F) because they strongly affect epibatidine affinity, and therefore allow us to deliberately alter the function of either the $\alpha\gamma$ or the $\alpha\delta$ site. These mutations were originally identified in ligand binding studies of the structural basis of carbamylcholine selectivity for the $\alpha\delta$ over the $\alpha\gamma$ site (Prince and Sine, 1996); the presence of both mutations in a single receptor nearly reverses the site selectivity for carbamylcholine. Curiously, however, for epibatidine the two mutations not only maintain the same site selectivity, but also markedly increase selectivity to

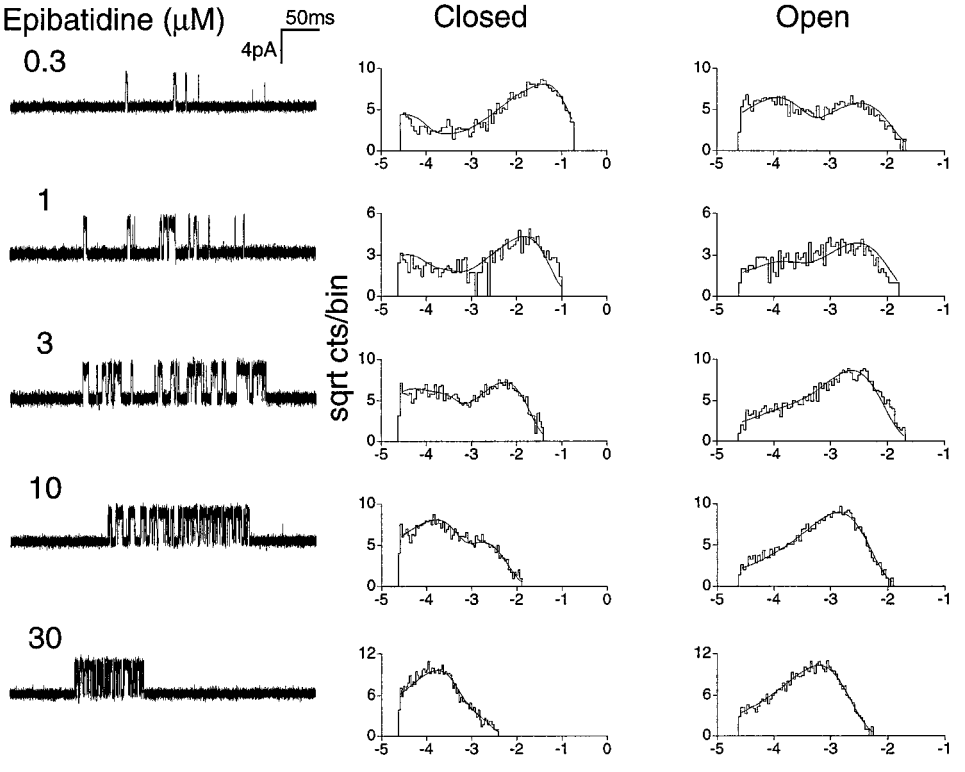

FIGURE 6 Single-channel responses of $\alpha_2\beta\delta\gamma$(K34S+F172I) receptors to epibatidine. Data were recorded at the indicated concentrations of epibatidine, using a final bandwidth of 9 kHz. The smooth curves through the open and closed dwell-time histograms are theoretical probability density functions calculated from the rate constants derived from Scheme 2. The fitted rate constants are given in Table 2.

approach 10000-fold. Carbamylcholine and epibatidine also differ in their state dependence of selectivity; carbamylcholine selects between sites in the resting but not the desensitized state, whereas epibatidine selects between sites in both the resting and desensitized states.

Differences between carbamylcholine and epibatidine selectivity suggest the following picture of how the non-α subunits contribute to the binding sites. Residues in multiple loops of the non-α subunits confer agonist selectivity. Some residues stabilize and others destabilize, but overall agonist selectivity is the sum of both types of interactions. Furthermore, selectivity depends on the state of the receptor; for a given agonist the resting state can be selective whereas the desensitized state is not, or both resting and desensitized states can be selective. Single-channel kinetic studies of the fetal receptor show that carbamylcholine selects between the two binding sites in the resting state (Zhang et al., 1995), whereas binding studies demonstrate that carbamylcholine does not distinguish between binding sites in the desensitized state (Prince and Sine, 1998b). The 30-fold selectivity of carbamylcholine for the resting state owes largely to residue differences at equivalent positions γK34/δS36 and γF172/δI178. When the receptor desensitizes, residues γK34/δS36 and γF172/δI178 no longer contribute to either affinity or selectivity, suggesting that they move out of range of carbamylcholine contact (Prince and Sine, 1996).

For epibatidine binding to the fetal receptor, both the resting and desensitized states are selective. Our single-channel data show that epibatidine selects between the binding sites in the resting state by 75-fold, and our binding studies show selectivity for sites in the desensitized state of 300-fold (Prince and Sine, 1998b). As we observe for carbamylcholine, the determinants γK34/δS36 and γF172/δI178 contribute to selectivity of the resting state, but not to selectivity of the desensitized state (Prince and Sine, unpublished). Thus the 300-fold selectivity of epibatidine for desensitized binding sites is due to determinants not yet identified. In the resting state, these unidentified determinants likely contribute significantly to epibatidine selectivity, perhaps as much as 300-fold, but the opposing contributions of γK34/δS36 and γF172/δI178 yield a net selectivity of 75-fold.

Our overall results demonstrate opposite site selectivity of ACh and epibatidine, indicating that the AChR channel can be opened regardless of the order in which the binding sites are occupied by agonist. Thus a scheme incorporating random association of agonist with the two binding sites (Scheme 2) provides a general description of AChR activation.

Open channel block also contributes to the P_{open} of epibatidine-activated receptors. Epibatidine is one of the most potent agonist channel blockers characterized thus far, with block dissociation constants (K_B) of $\sim$100 μM. For ACh, K_B is $\sim$6 mM (Sine and Steinbach, 1984; Wang et al., 1997). The open channel blocker, QX-222, which is not an agonist, interacts with adjacent turns of the M2 transmembrane domain (Charnet et al., 1990). QX-222 is thought to hydrogen bond via its quaternary ammonium group to an annulus of polar groups at position 6′ and via its aromatic group to an annulus of hydrophobic and aliphatic hydroxyl residues at position 10′ (position 1′ is the N-terminus of M2; Miller, 1989). Like QX-222, epibatidine contains a charged nitrogen and an aromatic moiety. Molecular modeling studies show that the internitrogen separation in epibatidine ranges from 4.7 Å to 5.7 Å (Bencherif et al., 1998), close to the separation between adjacent turns of an α-helix. Thus epibatidine may interact with the receptor channel in a manner similar to that of QX-222.

In summary, we describe molecular steps underlying activation fetal and adult muscle receptors by (−)-epibatidine. Epibatidine is a weak agonist at both receptor types because of reduced channel opening coupled with high-affinity open channel block. However, epibatidine shows unique site selectivity at the AChR, binding with low affinity to the $\alpha\delta$ interface in both receptor types. The unique properties of epibatidine make it a potentially useful probe in future structure-function studies.

This work was supported by National Institutes of Health Grant NS31744 (SMS) and by the Myasthenia Gravis Foundation (RJP).

REFERENCES

Akk, G., S. Sine, and A. Auerbach. 1996. Binding sites contribute unequally to the gating of mouse nicotinic αD200N acetylcholine receptors. *J. Physiol. (Lond.).* 496:185–196.

Bencherif, M., J. D. Schmitt, B. S. Bhatti, P. Crooks, W. S. Caldwell, M. E. Lovette, K. Fowler, L. Reeves, and P. M. Lippiello. 1998. The heterocyclic substituted pyridine derivative 2-azabicyclo[2.2.2]hept-5-ene (RJR-2429): a selective ligand at nicotinic acetylcholine receptors. *J. Pharmacol. Exp. Ther.* 284:886–894.

Blount, P., and J. P. Merlie. 1989. Molecular basis of the two nonequivalent ligand binding sites of the muscle nicotinic acetylcholine receptor. *Neuron.* 3:349–357.

Charnet, P., C. Labarca, R. J. Leonard, N. J. Vogelaar, L. Czyzyk, A. Gouin, N. Davidson, and H. A. Lester. 1990. An open-channel blocker interacts with adjacent turns of α-helices in the nicotinic acetylcholine receptor. *Neuron.* 2:87–95.

Fersht, A. R. 1985. Enzyme Structure and Mechanism. W. H. Freeman and Company, New York.

Gerzanich, V., X. Peng, F. Wang, G. Wells, S. Fletcher, and J. Lindstrom. 1995. Comparative pharmacology of epibatidine: a potent agonist for neuronal nicotinic receptors. *Mol. Pharmacol.* 48:774–782.

Maconochie, D. J., and J. H. Steinbach. 1998. The channel opening rate of adult- and fetal-type mouse muscle nicotinic receptors activated by acetylcholine. *J. Physiol. (Lond.).* 506:53–72.

Miller, C. 1989. Genetic manipulation of ion channels: a new approach to structure and mechanism. *Neuron.* 2:1195–1205.

Mishina, M., T. Takai, K. Imoto, M. Noda, T. Takahashi, S. Numa, C. Methfessel, and B. Sakmann. 1986. Molecular distinction between fetal and adult forms of muscle acetylcholine receptor. *Nature.* 321:406–411.

Neher, E., and J. H. Steinbach. 1978. Local anaesthetics transiently block currents through single acetylcholine-receptor channels. *J. Physiol. (Lond.).* 277:153–176.

Ohno, K., H-L. Wang, M. Milone, N. Bren, J. M. Brengman, S. Nakano, P. Quiram, J. N. Pruitt, S. M. Sine, and A. G. Engel. 1996. Congenital myasthenic syndrome caused by decreased agonist binding affinity due

to a mutation in the acetylcholine receptor ϵ subunit. *Neuron.* 17: 157–170.

Prince, R. J., and S. M. Sine. 1996. Molecular dissection of subunit interfaces in the acetylcholine receptor: identification of residues that determine agonist selectivity. *J. Biol. Chem.* 271:25770–25777.

Prince, R. J., and S. M. Sine. 1997. Determinants of agonist selectivity in the gamma and delta subunits of the nicotinic acetylcholine receptor (nAChR) affect the kinetics of activation. *Biophys. J.* 72:A334.

Prince, R. J., and S. M. Sine. 1998a. The ligand binding domains of the nicotinic acetylcholine receptor. *In* The Nicotinic Receptor: Current Views and Future Trends. F. J. Barrantes, editor. Landes Bioscience/ Springer Verlag, Georgetown, TX. 31–59.

Prince, R. J., and S. M. Sine. 1998b. Epibatidine binds with unique site and state selectivity to muscle nicotinic acetylcholine receptors. *J. Biol. Chem.* 273:7843–7849.

Qin, F., A. Auerbach, and F. Sachs. 1996. Estimating single-channel kinetic parameters from idealized patch clamp data containing missed events. *Biophys. J.* 70:264–80.

Sakmann, B., J. Patlak, and E. Neher. 1980. Single acetylcholine-activated channels show burst-kinetics in presence of desensitizing concentrations of agonist. *Nature.* 286:71–73.

Sine, S. M. 1993. Molecular dissection of subunit interfaces in the acetylcholine receptor: identification of residues that determine curare selectivity. *Proc. Natl. Acad. Sci. USA.* 90:9436–9440.

Sine, S. M., and T. Claudio. 1991. Gamma- and delta-subunits regulate the affinity and the cooperativity of ligand binding to the acetylcholine receptor. *J. Biol. Chem.* 266:19369–19377.

Sine, S. M., T. Claudio, and F. J. Sigworth. 1990. Activation of *Torpedo* acetylcholine receptors expressed in mouse fibroblasts: single channel current kinetics reveal distinct agonist binding affinities. *J. Gen. Physiol.* 96:395–437.

Sine, S. M., H-J. Kreienkamp, N. Bren, R. Maeda, and P. Taylor. 1995b. Molecular dissection of subunit interfaces in the acetylcholine receptor: identification of determinants of alpha-conotoxin M1 selectivity. *Neuron.* 15:205–211.

Sine, S. M., K. Ohno, C. Bouzat, A. Auerbach, M. Milone, N. J. Pruitt, and A. G. Engel. 1995a. Mutation of the acetylcholine receptor alpha subunit causes a slow-channel myasthenic syndrome by enhancing agonist binding affinity. *Neuron.* 15:229–239.

Sine, S. M., and J. H. Steinbach. 1984. Agonists block currents through acetylcholine receptor channels. *Biophys. J.* 45:175–185.

Sine, S. M., and J. H. Steinbach. 1987. Activation of acetylcholine receptors on clonal mammalian BC3H-1 cells by high concentrations of agonist. *J. Physiol. (Lond.).* 385:325–359.

Sullivan, J. P., M. W. Decker, J. D. Brioni, D. Donnely-Roberts, D. J. Anderson, A. W. Bannon, C. Kang, P. Adems, M. Piattoni-Kaplan, M. J. Buckley, M. Gopalakrishnan, M. Williams, and S. P. Arneric. 1994. (±)-Epibatidine elicits a diversity of in vitro and in vivo effects mediated by nicotinic acetylcholine receptors. *J. Pharmacol. Exp. Ther.* 271:624–631.

Wang, H-L., A. Auerbach, N. Bren, K. Ohno, A. G. Engel, and S. M. Sine. 1997. Mutation in the M1 domain of the acetylcholine receptor α subunit decreases the rate of agonist dissociation. *J. Gen. Physiol.* 109:757–766.

Zhang, Y., J. Chen, and A. Auerbach. 1995. Activation of recombinant mouse acetylcholine receptors by acetylcholine, carbamylcholine and tetramethylammonium. *J. Physiol. (Lond.).* 486:189–206.